This is an open access article published under an ACS AuthorChoice License, which permits copying and redistribution of the article or any adaptations for non-commercial purposes.

Langmuir

Article

pubs.acs.org/Langmuir

Stretch-Activated Pore of the Antimicrobial Peptide, Magainin 2

Mohammad Abu Sayem Karal,[†] Jahangir Md. Alam,[‡] Tomoki Takahashi,[§] Victor Levadny,[†,∥] and Masahito Yamazaki*[,†,‡,§]

[†]Integrated Bioscience Section, Graduate School of Science and Technology, [‡]Nanomaterials Research Division, Research Institute of Electronics, and [§]Department of Physics, Faculty of Science, Shizuoka University, Shizuoka, 422-8529, Japan

[∥]Theoretical Problem Center of Physico-Chemical Pharmacology, Russian Academy of Sciences, Kosugina, 4, 117977, Moscow, Russia

Supporting Information

ABSTRACT: Antimicrobial peptide magainin 2 forms pores in lipid membranes and induces membrane permeation of the cellular contents. Although this permeation is likely the main cause of its bactericidal activity, the mechanism of pore formation remains poorly understood. We therefore investigated in detail the interaction of magainin 2 with lipid membranes using single giant unilamellar vesicles (GUVs). The binding of magainin 2 to the lipid membrane of GUVs increased the fractional change in the area of the membrane, δ, which was proportional to the surface concentration of magainin 2, X. This indicates that the rate constant of the magainin 2-induced two-state transition from the intact state to the pore state greatly increased with an increase in δ. The tension of a lipid membrane following aspiration of a GUV also activated magainin 2-induced pore formation. To reveal the location of magainin 2, the interaction of carboxyfluorescein (CF)-labeled magainin 2 (CF-magainin 2) with single GUVs containing a water-soluble fluorescent probe, AF647, was investigated using confocal microscopy. In the absence of tension due to aspiration, after the interaction of magainin 2 the fluorescence intensity of the GUV rim due to CF-magainin 2 increased rapidly to a steady value, which remained constant for a long time, and at 4−32 s before the start of leakage of AF647 the rim intensity began to increase rapidly to another steady value. In contrast, in the presence of the tension, no increase in rim intensity just before the start of leakage was observed. These results indicate that magainin 2 cannot translocate from the outer to the inner monolayer until just before pore formation. Based on these results, we conclude that a magainin 2-induced pore is a stretch-activated pore and the stretch of the inner monolayer is a main driving force of the pore formation.

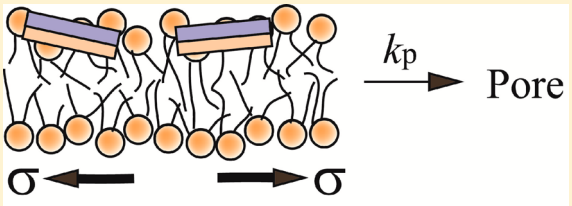

1. INTRODUCTION

Antimicrobial peptides (AMPs) with bactericidal activity have been discovered in, and isolated from, a wide variety of organisms, including amphibians, invertebrates, plants, and mammals.[1−3] Among these AMPs, magainin 2, first isolated from the African clawed frog *Xenopus laevis*,[4,5] has been extensively investigated. Magainin 2 composed of all-D-amino acids has the same antibacterial activity as that of natural magainin 2 composed of all-L-amino acids.[6] Since no specific interaction of magainin 2 with chiral receptors or proteins is required for its antibacterial activity, magainin 2 likely targets the lipid membrane regions of bacterial membranes. Magainin 2 is a positively charged peptide composed of 23 amino acids, and thus can bind selectively to the negatively charged outer monolayer of the bacterial cytoplasmic membrane via electrostatic attraction.[1] When magainin 2 binds to a lipid membrane, it forms an α-helix at the lipid membrane interface, parallel to the membrane surface.[7,8] To elucidate the mechanism of the bactericidal activity of magainin 2, the interaction of magainin 2 with lipid membranes was previously investigated using a suspension of many small liposomes such as large unilamellar vesicles (LUVs).[9−12] These studies indicate that magainin 2 induces leakage of the internal contents, such as water-soluble fluorescent probes, from the inside of LUVs, suggesting that magainin 2 induces pores in lipid membranes. However, the elementary processes underlying magainin 2-induced pore formation were not clearly revealed, since data obtained using the LUV suspension method provide only average values of the physical properties of all the LUVs which stay in different elementary processes.[13]

Giant unilamellar vesicles (GUVs) of lipid membranes with diameters greater than 10 μm have an advantage over the LUVs because shapes and fluorescent probes of GUVs can be visualized using optical microscopes.[14−18] We have recently developed the single GUV method for investigation on the interaction of peptides/proteins with lipid membranes.[13,19−25] In this method, changes in the structure and physical properties of a single GUV that are induced by interactions with peptides/proteins are observed as a function of time and spatial coordinates. The same experiments are then carried out using many "single GUVs" and their results of the changes in the physical properties of single GUVs are statistically analyzed

Received: August 19, 2014
Revised: February 28, 2015
Published: March 6, 2015

 © 2015 American Chemical Society

DOI: 10.1021/la503318z
Langmuir 2015, 31, 3391−3401

over many "single GUVs". Thereby, the single GUV method can reveal the details of elementary processes of individual events, and allow calculation of their kinetic constants. Using this method, we obtained new information on the interaction of magainin 2 as follows. During the interaction of magainin 2 with a single GUV encapsulating a fluorescent probe, calcein, a rapid reduction in the fluorescence intensity inside the GUV occurred stochastically, indicating that magainin 2 molecules bound to the GUV induced stochastic pore formation in the GUV membrane and that calcein leaked through these pores. From analysis of the time course of the fraction of intact (no leakage of fluorescent probe) GUVs among all the examined GUVs, we obtained the rate constant, k_p, of the irreversible two-state transition from the state of intact GUV (i.e., nonleaky GUV) where magainin 2 molecules bound to the membrane interface of the outer monolayer to the state of the pore through which internal contents of the GUV are leaking or have completely leaked (i.e., leaking or leaked GUV), and defined it as the rate constant of the magainin 2-induced pore formation.[20,21] The values of k_p greatly depend on the negatively charged dioleoylphosphatidylglycerol (DOPG) concentration in a mixture of DOPG and electrically neutral dioleoylphosphatidylcholine (DOPC).[21] We found that the surface concentration of magainin 2 in the outer monolayer of a GUV is the main determinant of k_p, which increases with an increase in the surface concentration at and above its critical value.[21] The rate constants of membrane permeation (or leakage) through the magainin 2-induced pores, k_{mp}, and the time course of k_{mp} were obtained.[22] These data provide information on the kinetic pathway of magainin 2-induced pore formation in lipid membranes, which supports the toroidal structure model of the magainin 2-induced pore.[26−28] Based on these results, we proposed that the binding of magainin 2 to the outer monolayer induces tension in the inner monolayer, which plays a key role in magainin 2-induced pore formation.[22]

In this report, to reveal the mechanism of magainin 2-induced pore formation in more detail, we investigated the interaction of magainin 2 with lipid membranes using single GUVs. First, we examined the magainin 2-induced change in area of lipid membranes of single DOPG/DOPC-GUVs. Then, we investigated the effect of tension caused by aspiration of a GUV on magainin 2-induced pore formation. These results indicate that stretching a lipid membrane activates magainin 2-induced pore formation. To elucidate the relationship between stretching and pore formation, it is important to determine the location of magainin 2 in a GUV membrane during the interaction of magainin 2 with a single GUV. For this purpose, we investigated the interaction of magainin 2 labeled with a fluorescent probe, carboxyfluorescein, (CF-magainin 2) with a single GUV using confocal laser scanning microscopy (CLSM) by the method developed in our previous paper.[23] Based on these results, we discuss the mechanism underlying magainin 2-induced pore formation.

2. MATERIALS AND METHODS

2.1. Chemicals. DOPG and DOPC were purchased from Avanti Polar Lipids Inc. (Alabaster, AL). Alexa Fluor 647 hydrazide (AF647) and 5-(and 6)-carboxyfluorescein (CF) succinimidyl ester were purchased from Invitrogen Inc. (Carlsbad, CA). Bovine serum albumin was purchased from Wako Pure Chemical Industry Ltd. (Osaka, Japan). Magainin 2 was synthesized and purified as described in our previous paper.[20] CF-labeled magainin 2 (i.e., CF-magainin 2) was synthesized using a standard method.[23] The measured mass of CF-magainin 2 was 2824 ± 1 Da, which corresponds to the calculated mass. CF-magainin 2 concentrations in a buffer were determined by its absorbance using the molar absorption coefficient of CF (81 000) at 492 nm.

2.2. GUV Preparation and Its Observation. 40%DOPG/60%DOPC-GUVs and 30%DOPG/70%DOPC-GUVs (where % indicates mole %) were prepared by the natural swelling method.[20] 20 μL Milli-Q water was added into a dry lipid film in the glass vial, and the mixture was incubated around 45 °C for ∼7 min (prehydration), and then incubated with 1 mL of buffer A (10 mM PIPES, pH 7.0, 150 mM NaCl, and 1 mM EGTA) containing 0.10 M sucrose for 2 to 3 h at 37 °C. To obtain a purified GUV suspension, smaller vesicles and untrapped fluorescent probes were removed using the membrane filtering method;[29] after centrifugation, the supernatant was filtered through a nuclepore membrane with 10-μm-diameter pores (Whatman, GE Healthcare, UK, Ltd., Buckinghamshire, England) in buffer A containing 0.10 M glucose for 1 h at a flow rate of 1 mL/min at room temperature (20−25 °C), and the suspension which was not passed through the filter was collected and used for following experiments as a purified GUV suspension. To prepare GUVs containing AF647, we used buffer A containing 6 μM AF647 in the above procedure. After the purification, a GUV suspension (∼300 μL) was transferred into a handmade microchamber, which had been formed on a glass slide by inserting a U-shaped silicone-rubber spacer (for experiments using a micropipet)[13] or two parallel-deposited bar-shaped silicon-rubber spacer (for experiments using two micropipets) between a coverslip and the glass slide. To prevent strong interaction between the glass surface and GUVs, the inside of the microchamber was coated with 0.10% (w/v) BSA in the same buffer for the experiments.[13] The GUVs were observed using an inverted fluorescence, differential interference contrast (DIC) microscope (IX-71, Olympus, Tokyo, Japan) or a CLSM (FV1000-D, Olympus, Tokyo, Japan) with 60× objective at 25 ± 1 °C controlled by a stage thermocontrol system (Thermoplate, Tokai Hit, Shizuoka, Japan).

2.3. Measurement of Fractional Change in the Area of a GUV Induced by Binding of Magainin 2 to the Lipid Membrane. A standard micropipet aspiration method[15,30] was used to measure the fractional change in the area of a single GUV. A single GUV was held at the tip of a micropipet A with a diameter of ∼10 μm, which was coated with 0.50% (w/v) BSA in buffer A containing 0.10 M glucose, for a few minutes by applying aspiration pressure, ΔP (= $P_{out} - P_{in}$, where P_{out} and P_{in} are the pressure of the outside and the inside of a micropipet, respectively) (Figure 1A).[13] ΔP was adjusted so that the tension of the GUV membrane, σ, was 0.50 mN/m. σ can be described as a function of ΔP as follows:[15]

$$\sigma = \frac{\Delta P d_p}{4(1 - d_p/D_V)} \quad (1)$$

where d_p is the internal diameter of the micropipet and D_V is the diameter of the spherical cap segments (in the outside of the micropipet) of the aspirated GUV. Then, magainin 2 solution was continuously added from another micropipet B with a diameter of ∼20 μm into the vicinity of the GUV. The distance between the GUV and the tip of the micropipet B was ∼40 μm, and ΔP of the micropipet B was −30 Pa. The measurement of ΔP was done using a differential pressure

DOI: 10.1021/la503318z
Langmuir 2015, 31, 3391−3401

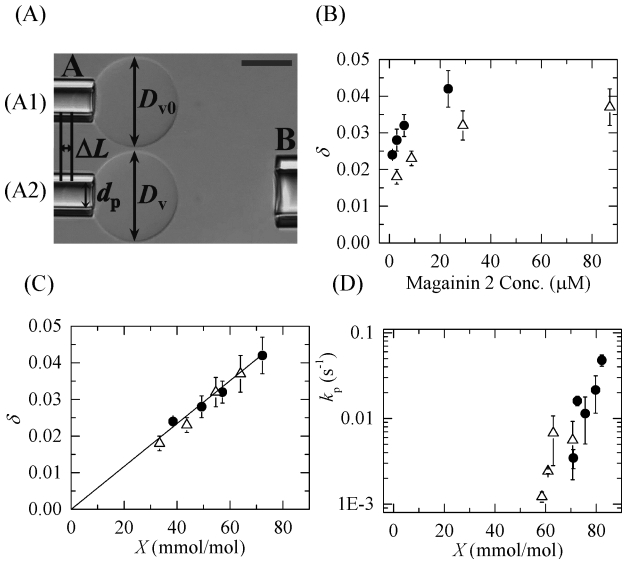

Figure 1. Effect of binding of magainin 2 to a GUV on its area and on the rate constant of magainin 2-induced pore formation. (A) (A1) DIC image of a GUV fixed at the tip of a micropipet A using a small aspiration pressure. (A2) Magainin 2 solution was continuously added from another micropipet B into the vicinity of the GUV shown in (A1). d_p is the internal diameter of the micropipet, and D_V and D_{V0} are the diameter of the spherical cap segments of the aspirated GUV after and before the interaction with magainin 2, respectively. The bar corresponds to 20 μm. (B) Fractional change in area, δ, of single GUVs induced by the binding of magainin 2 as a function of the magainin 2 concentration in buffer A (μM) in the vicinity of a GUV. The same experiment was repeated with ~10 GUVs to provide an average value of δ and the standard error for each magainin 2 concentration. (C) Dependence of δ on the magainin 2 surface concentration at the membrane interface, X (mmol/mol). (●) 40% DOPG/60%DOPC-GUV, and (Δ) 30%DOPG/70%DOPC-GUV. (D) Rate constant of magainin 2-induced two-state transition from the intact state to the pore state, k_p, as a function of X. (●) 40% DOPG/60%DOPC-GUV, and (Δ) 30%DOPG/70%DOPC-GUV. The re-evaluated values of X were used. Average values and standard errors are shown.

transducer (DP15, Validyne, CA), pressure amplifier (PA501, Validyne, CA), and a digital multimeter.[13] Glass micropipets were prepared by pulling 1.0 mm glass capillary composed of borosilicate glass (G-1, Narishige, Tokyo, Japan) using a puller (PP-83 or PC-10, Narishige, Tokyo, Japan).[13] Magainin 2 concentrations in the vicinity of the GUV were determined by the method described in section 2.5.

The fractional change in the area of the GUV membrane is $\delta = \Delta A/A_0$, where A_0 is the area of a GUV before the interaction with magainin 2 and ΔA is the change in the area of the GUV membrane after the interaction with magainin 2. Several parameters are required to obtain δ (Figure 1A). One parameter is the change in the projection length, $\Delta L = L_{eq} - L_0$, where L_{eq} and L_0 are the projection length of the GUV at equilibrium after and before the interaction with magainin 2, respectively. The equation for δ without assuming constant volume is given by[31]

$$\delta = \frac{\Delta A}{A_0} = \frac{\Delta L d_p + D_v^2 - D_{v0}^2}{D_{v0}^2} \quad (2)$$

where D_V and D_{V0} are the diameter of the spherical cap segments of the aspirated GUV at equilibrium after and before the interaction with magainin 2, respectively. The DIC images of the GUV were recorded by CCD (CS230B, Olympus, Tokyo, Japan), and the length of the parameters (L_{eq}, L_0, D_V, and D_{V0}) were measured using video converter software (Wondershare, Tokyo, Japan). In this experimental system, during addition of magainin 2 solution, the inside of micropipet A did not contain magainin 2 solution. We estimated the fraction of the area of a GUV membrane inside the micropipet A among the entire area of the GUV membrane before the interaction of magainin 2 (i.e., before its addition), which was 8.8 ± 0.6 (%). During the interaction of magainin 2, the area of the GUV increased, and thereby the fraction of the GUV membrane inside a micropipet increased. However, the magainin 2 molecules bound with the membrane surface also transferred into the inside of the micropipet with the part of the GUV membrane, and thereby we can neglect the contribution of the fraction of the GUV membrane increased by the interaction of magainin 2. Therefore, the values of the fraction of area change in Figure 1B,C were underestimated by ~9%.

2.4. Effect of the Tension of Lipid Membranes on Magainin 2-Induced Pore Formation. First, a single GUV was held at the tip of a micropipet A with a diameter of ~10 μm using a small aspiration pressure (the tension of the membrane was 0.50 mN/m) for a few minutes, then magainin 2 solution was continuously added from another micropipet B with a diameter of ~20 μm into the vicinity of the GUV for 40 s until steady binding of magainin 2 to the GUV membrane was attained. Next, the GUV was rapidly (~10 s) aspirated to a specific value of tension, which was kept for a specific time. During the application of constant tension the GUV was suddenly aspirated into the micropipet completely as a result of pore formation. The time of pore formation was defined as the time when the GUV was completely aspirated; the time resolution was less than 1 s. Note that the time of pore formation was started to count when the tension of the GUV reached the specific constant one. When the same experiment was repeated with many GUVs, pore formation was found to occur stochastically. To analyze this stochastic phenomena, the time-course of the fraction of intact GUVs without complete aspiration (i.e., pore formation) among all the examined GUVs, $P_{intact}(t)$, was obtained. From the fitting of $P_{intact}(t)$ to a single exponential decay function, the rate constant of magainin 2-induced pore formation in the presence of constant tension was obtained. The fraction of GUVs which were aspirated into the micropipet before attaining a specific value of tension ranged from 2% to 16% of all the examined GUVs, which increased with an increase in tension (its average was 9 ± 2%). We excluded this fraction from the calculation of $P_{intact}(t)$, and thereby the errors of $P_{intact}(t)$ and the rate constant of pore formation were ~9%. Magainin 2 concentrations in the vicinity of the GUV were determined by the method described in section 2.5. We estimated the fraction of the area of a GUV membrane inside a micropipet among the entire area of the GUV membrane before the interaction of magainin 2 (i.e., before its addition), which was 8.8 ± 0.6 (%). Thereby the values of magainin 2 concentration in Figure 2 were overestimated by ~9%. The typical size range of GUVs was 25−32 μm in diameter.

It is worth noting that when we used another method (i.e., first a GUV was held at a specific tension such as 3.0 mN/m, and then magainin 2 solution was added into the vicinity of the GUV), two-phase decay (a rapid and a slow decay) of $P_{intact}(t)$ was observed. It means that it was not possible to fit the time

DOI: 10.1021/la503318z
Langmuir 2015, 31, 3391−3401

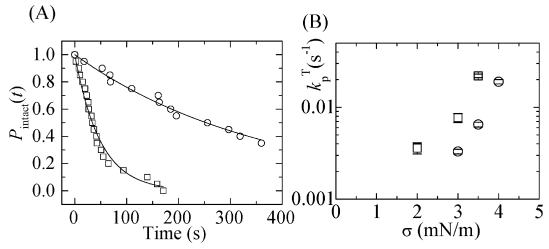

Figure 2. Effect of tension caused by an external force on magainin 2-induced pore formation in single GUVs. (A) Time course of the fraction of intact 40%DOPG/60%DOPC-GUVs in the presence of 5.8 μM magainin 2 among all the examined GUVs, $P_{intact}(t)$, following application of tension, σ: (○) 2.0, (□) 3.5 mN/m. Twenty single GUVs were examined in each experiment. The solid line represents the best fit curve of eq 3. (B) Dependence of k_p^T on tension. (□) 40% DOPG/60%DOPC-GUVs in the presence of 5.8 μM magainin 2, and (○) 30%DOPG/70%DOPC-GUVs in the presence of 29 μM magainin 2. The average values and standard error for k_p^T at each tension were determined from 3 independent experiments using 20 GUVs.

course of P_{intact} by a single exponential curve. This is probably because the nonequilibrium effect of the binding of magainin 2 to the membrane can induce a transient, large increase in the tension of the GUV membrane. We therefore did not use this method.

2.5. Relationship between the Location of Magainin 2 and Magainin 2-Induced Pore Formation. We investigated the interaction of CF-magainin 2 with single 40%DOPG/60% DOPC-GUVs containing AF647 using a CLSM at 25 ± 1 °C controlled by a stage thermocontrol system.[23] For CLSM measurement, fluorescence images of AF647 (excited by a laser at λ = 633 nm) and of CF-magainin 2 (excited by a laser at λ = 488 nm) were obtained using a 60× objective (UPLSA-PO060X0, Olympus).[23] The CF-magainin 2/magainin 2 solution containing 0.16 μM CF-magainin 2 was continuously provided to the vicinity of a GUV through a micropipet with a diameter of ∼20 μm. The distance between the GUV and the tip of the micropipet was ∼70 μm, and ΔP = −30 Pa. The fluorescence intensities of images obtained by the CLSM were measured using the software of the CLSM (*Fluoview* v 4.1, Olympus, Tokyo, Japan). The fluorescence intensity of the rim of the GUV (i.e., the GUV membrane) was measured using a modified method of ref 23 as follows (see the details in Supporting Information (SI)). First, 8 lines were drawn from the center of the GUV to its outside for each GUV image (Figure S2). We obtained the fluorescence intensities of CF-magainin 2 and AF647 along a line and then subtracted the background intensity (i.e., the fluorescence intensity of the same buffer) from these intensities to obtain a line profile of the fluorescence intensities.[32] Then, 8 line profiles were superimposed to obtain an average line profile. We defined the edge of the GUV, where the fluorescence intensity of AF647 inside the GUV greatly decreased, as the rim of the GUV (indicated by a black arrow in Figures S3 and S4). We always observed a sharp, largest peak at the edge of the GUV (e.g., Figures S3 and S4). Thereby the fluorescence intensity of CF-magainin 2 at this edge was defined as that of CF-magainin 2 at the rim.

To obtain magainin 2 concentrations in the vicinity of the GUV, the average fluorescence intensities of the outside vicinity of the GUV were obtained by averaging the intensities of all the points inside the 8 circles with a diameter of ∼10 μm near the GUV and then subtracting the background intensity. Using the calibration curve (the fluorescence intensity vs CF-magainin 2 concentration, Figure S1), we obtained the CF-magainin 2/magainin 2 concentrations in the vicinity of the GUV (see the details in SI).

2.6. Simultaneous Measurement of the Time Course of Magainin 2-Induced Change in the Area of the Membrane, Magainin 2 Concentration in the Membrane, and Membrane Permeation of AF647. A CLSM at 25 ± 1 °C with a stage thermocontrol system was used.[23] A single 40%DOPG/60%DOPC-GUV containing AF647 was held at the tip of a micropipet A with a diameter of ∼10 μm using a small aspiration pressure (the tension of the membrane was 0.50 mN/m), then CF-magainin 2/magainin 2 solution was continuously added from another micropipet B with a diameter of ∼20 μm into the vicinity of the GUV. Magainin 2 concentrations in the vicinity of the GUV were determined by the method described in section 2.5. The distance between the GUV and the tip of the micropipet was ∼40 μm. The fractional change in the area of the GUV membrane, $\delta = \Delta A/A_0$, was obtained using eq 2. The fluorescence intensity of the rim of the GUV was measured using the method described in section 2.5.

3. RESULTS

3.1. Binding of Magainin 2 to the Lipid Membrane of a Single GUV Induces an Increase in Its Area. First, we investigated the effects of the binding of magainin 2 to the membrane of a 40%DOPG/60%DOPC-GUV on its area. A single GUV was held at the tip of a micropipet A in buffer A using a small aspiration pressure (the tension on the membrane was 0.50 mN/m) (Figure 1A1) while magainin 2 solution was continuously added from another micropipet B into the vicinity of the GUV (Figure 1A2). As magainin 2 interacted with the GUV, the change in projection length of the GUV inside the micropipet, ΔL, increased with time, and then reached a steady value in less than 1 min. Using eq 2, we calculated the steady fractional change of the area of the GUV membrane, $\delta = \Delta A/A_0$. Figure 1B (●) shows that δ increased with an increase in magainin 2 concentration in the buffer, and that δ = 0.042 ± 0.005 (n = 9) at 23 μM magainin 2. A similar result was obtained for 30%DOPG/70%DOPC-GUVs (Figure 1B, Δ).

Next, we analyzed quantitatively the relationship between δ and the magainin 2 surface concentration at the membrane interface, which is expressed by the molar ratio of magainin 2 bound to the membrane interface to lipids in the outer monolayer, X (mol/mol). As described in our previous paper,[21] using the intrinsic binding constant of magainin 2 to lipid membranes, K_{int}^{mag}, and the Poisson-Boltzmann equation, we can convert the magainin 2 concentration in the buffer C_{eq}^{mag} into X. Here, using the re-evaluated values of K_{int}^{mag} (i.e., 350 for 40% DOPG/60%DOPC and 320 for 30%DOPG/70%DOPC) (for further details, see SI), we converted C_{eq}^{mag} into X. Figure 1C shows that $\delta \propto X$, i.e., $\delta = aX$, where a is the proportionality constant and a = 0.58 ± 0.01. We can reasonably consider that in the membrane, the magainin 2 molecule inserts into the interface of the outer monolayer due to its high interfacial hydrophobicity[33] and pushes the lipid headgroups laterally to increase the area of the outer monolayer.[20] This can explain the experimental result that $\delta \propto X$.

Using the re-evaluated values of K_{int}^{mag} and the corrected magainin 2 concentrations in the vicinity of the GUV by the method described in section 2.5, we revised the figure of the rate constant of the magainin 2-induced two-state transition

DOI: 10.1021/la503318z
Langmuir 2015, 31, 3391−3401

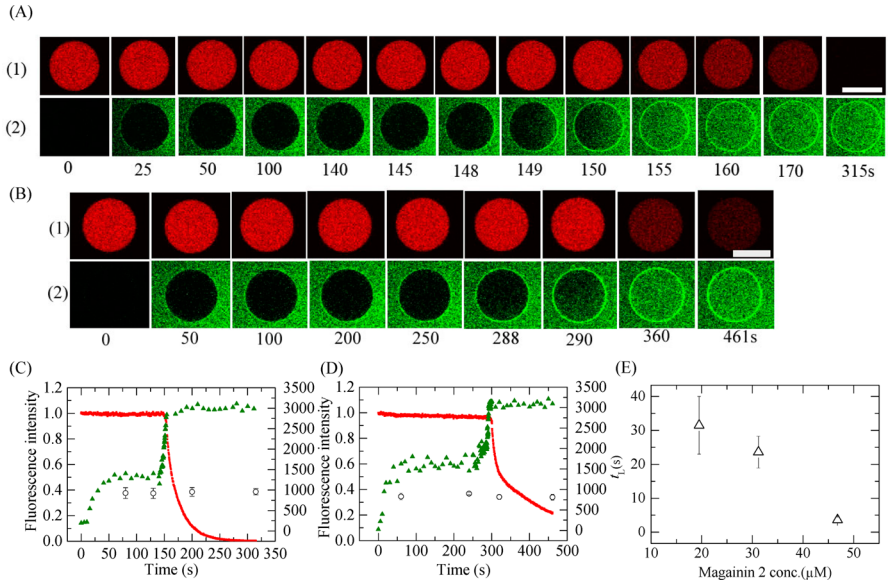

Figure 3. Membrane permeation of AF647 and location of CF-magainin 2 in single 40%DOPG/60%DOPC-GUVs induced by 31 μM CF-magainin 2/magainin 2 (A) and 20 μM CF-magainin 2/magainin 2 (B). CLSM images of (1) AF647 and (2) CF-magainin 2. The numbers below each image show the time in seconds after initiation of CF-magainin 2/magainin 2 addition. The bar corresponds to 30 μm. (C) and (D) show time course of the change in fluorescence intensity of the GUV shown in (A) and in (B), respectively. The solid red line corresponds to the fluorescence intensity of AF647 inside the GUV, which is expressed as normalized fluorescence intensity (left axis of C and D), FI = $I(t)/I(0)$, where $I(t)$ and $I(0)$ are the fluorescence intensity of AF647 inside the GUV at time = t (i.e., the time after the addition of magainin 2 started) and time = 0 (i.e., the time when the addition of magainin 2 started). The green triangles correspond to the fluorescence intensity of CF-magainin 2 in the rim of the GUV (right axis of C and D). The circles correspond to the fluorescence intensity of the outside vicinity of the GUV. (E) Magainin 2 concentration dependence of the average lag time between when the rim intensity started to increase and the start of membrane permeation, t_L. Average values and standard error of t_L were determined from 2 independent experiments using 5−13 GUVs.

from the intact state to the pore state, k_p, vs X which was reported previously[21] (Figure 1D). It indicates that k_p greatly increases with an increase in X. Therefore, the above results clearly show that k_p increases greatly with an increase in area of the GUV membrane.

3.2. Effect of the Tension of the Lipid Membrane on Magainin 2-Induced Pore Formation. To reveal the role of tension in magainin 2-induced pore formation, we investigated the effect of tension caused by aspiration of a GUV.[30] For this purpose, in the presence of magainin 2, we increased the lateral membrane tension of the GUV to a certain value and observed pore formation in the GUV. A single 40%DOPG/60%DOPC-GUV was held at the tip of a micropipet A using a small aspiration pressure (the tension on the membrane was 0.50 mN/m) (Figure 1A1) for a few minutes and then a magainin 2 solution was continuously added for 40 s from another micropipet B into the vicinity of the GUV (magainin 2 concentration in the vicinity of the GUV was 5.8 μM) to attain steady binding of magainin 2 to the membrane (Figure 1A2). Note that the rate constant of 5.8 μM magainin 2-induced pore formation in 40% DOPG/60%DOPC-GUVs in the absence of tension was too small to be determined accurately.[21] We then rapidly (~10 s) increased the aspiration pressure to a constant tension of 2.0 mN/m and held this tension for a specific time in the presence of 5.8 μM magainin 2 in the vicinity of the GUV. During application of this tension, magainin 2 solution was continuously added, hence the magainin 2 concentration near the GUV remained constant. After a period of time, the GUV was suddenly aspirated into the micropipet completely due to pore formation in the GUV membrane. Note that a tension less than 4.0 mN/m cannot induce a pore in a 40%DOPG/60% DOPC-GUV in the absence of magainin 2.[30] When the same experiment was repeated with 20 single GUVs, pore formation was found to occur stochastically. The time-course of the fraction of intact GUVs without complete aspiration (i.e., pore formation) among all the examined GUVs, $P_{intact}(t)$, could be fit well by a single exponential decay function as follows (○ in Figure 2A)

$$P_{intact}(t) = \exp(-k_p^T t) \quad (3)$$

where k_p^T is the rate constant of magainin 2-induced pore formation in the presence of constant tension in the membrane caused by aspiration of a GUV, and t is the time that the constant tension was applied to the GUV (constant tension began at t = 0). From this fitting, the value of k_p^T was determined to be 2.7 × 10^{-3} s^{-1}. Using the same method we investigated the effects of various tensions, and found that k_p^T increased greatly with tension (Figure 2B, □). A similar result was obtained for 30%DOPG/70%DOPC-GUVs interacting 29 μM magainin 2 (Figure 2B, ○). Note that a tension less than 4.5 mN/m cannot induce a pore in a 30%DOPG/70%DOPC-GUV in the absence of magainin 2. As shown in Figure 2B, the values of k_p^T for 40%DOPG/60%DOPC-GUVs interacting 5.8 μM magainin 2 (X = 57 mmol/mol) were larger than those of 30%DOPG/70%DOPC-GUVs interacting 29 μM magainin 2 (X = 55 mmol/mol) at the same tensions. For both conditions, X values are similar and the corresponding δ values are the same (δ = 0.032) (Figure 1C). However, as reported in our previous paper,[30] the rate constant of tension-induced pore formation increases with an increase in the electrostatic interactions due to the surface charges of lipid membranes, indicating that the mechanical stability of lipid membranes decreases with an increase in the electrostatic interactions. This can reasonably explain the difference of k_p^T for the different

DOI: 10.1021/la503318z
Langmuir 2015, 31, 3391−3401

membranes. These results clearly show that tension due to an external force activates magainin 2-induced pore formation, indicating that stretching of the lipid membrane activates magainin 2-induced pore formation, and that k_p^T increases with an increase in the stretch of a lipid membrane.

3.3. Relationship between the Location of Magainin 2 and the Membrane Permeation of AF647. To understand the mechanism of magainin 2-induced pore formation in lipid membranes, the information on location of magainin 2 in a GUV is important. It has been reported that some peptides can translocate from the outer monolayer to the inner monolayer before pore formation.[23,34,35] However, it is generally considered that translocation of peptides/proteins across lipid bilayers depends on the properties of peptides/proteins (such as size and charges) and those of lipid bilayer (such as thickness and fluidity). Thereby it is reasonably considered that many peptides/proteins cannot translocate across specific lipid bilayers without pores whose diameter is larger than that of peptide/proteins. It is therefore necessary to elucidate the relationship between the location of magainin 2 in a GUV and magainin 2-induced pore formation. For this purpose, we investigated the interaction of CF-magainin 2/magainin 2 with single 40%DOPG/60%DOPC-GUVs containing a fluorescent probe, AF647, using CLSM. Figure 3A shows a typical result from the interaction of 31 μM CF-magainin 2/magainin 2 with single GUVs. A fluorescence microscope image of a GUV (Figure 3A (1)) shows a high concentration of AF647 inside the GUV. During the addition of the CF-magainin 2/magainin 2 solution, the fluorescence intensity inside the GUV remained essentially constant over the first 148 s, after which the fluorescence intensity gradually decreased (Figure 3A (1) and red line in Figure 3C). After 270 s, the fluorescence intensity due to AF647 was zero, although a fluorescence microscope image of the same GUV imaged using CF-magainin 2 fluorescence (Figure 3A (2)) shows that the GUV was spherical and not broken. As discussed in our reports on magainin 2,[20,21] the decrease in fluorescence intensity results from the membrane permeation of AF647 from the GUV through magainin 2-induced pores in the membrane. Thus, the time at which the fluorescence intensity began to rapidly decrease (t = 149 s) corresponds to the time when the membrane permeation of AF647 started (for further details, see SI). On the other hand, a fluorescence microscope image of the GUV, obtained by imaging CF-magainin 2 (Figure 3A2), shows that the fluorescence intensity of the rim of the GUV corresponding to the GUV membrane (i.e., the rim intensity) rapidly increased to a steady value, I_1, at around t = 50 s, then remained constant until t = 140 s (green triangle in Figure 3C), which was larger than the fluorescence intensity of the outside of the GUV (○ in Figure 3C). This result indicates that the steady binding of magainin 2 between the aqueous phase and the GUV membrane was attained around ∼50 s and that the surface concentration of CF-magainin 2/magainin 2, X, remained constant for ∼90 s (suggesting that δ was constant during these ∼90 s because $\delta = aX$). At t = 140 s (9 s before the start of membrane permeation), the rim intensity started to increase and after ∼15 s reached another steady value, I_2. Similar rim intensity results were obtained for other GUVs (n = 13). The rim intensity rapidly increased to a steady value, I_1, in less than ∼50 s, then remained constant for a long time (40−240 s). Before the start of membrane permeation, the rim intensity rapidly started to increase from I_1, and then finally reached another steady value, I_2. The average value of I_2/I_1 was 2.1 ± 0.1 (n = 13). The average lag time between the time when the rim intensity started to increase and the time when membrane permeation commenced, t_L, was 24 ± 5 s. The attachment of CF to magainin 2 may change the behavior of the peptide. However, the rate constant of 31 μM CF-magainin 2-induced pore formation in 40%DOPG/60%DOPC-GUVs was only 2.1 times larger than that of 31 μM magainin 2-induced pore formation. Thereby, as an approximation, we can consider that CF-magainin 2 behaves similarly to magainin 2.

We repeated the experiment corresponding to Figure 3A using various concentrations of CF-magainin 2/magainin 2. Figure 3B shows the result of 20 μM CF-magainin 2/magainin 2 (containing 0.16 μM CF-magainin 2). The membrane permeation of AF647 started at 297 s (red line in Figure 3D). The rim intensity rapidly increased to a steady value, I_1, at around t = 50 s, then remained constant for ∼220 s, and at t = 267 s (30 s before the start of membrane permeation), the rim intensity started to increase to another steady value, I_2 (green triangle in Figure 3D). The average value of t_L was 32 ± 9 s, and that of I_2/I_1 was 1.8 ± 0.1 (n = 5). The rim intensities were larger than those for 31 μM CF-magainin 2/magainin 2 because the fraction of CF-magainin 2 in 20 μM CF-magainin 2/magainin 2 (0.80 mol %) is larger than that of 31 μM CF-magainin 2/magainin 2 (0.50 mol %). In the case of 47 μM CF-magainin 2/magainin 2 (containing 0.16 μM CF-magainin 2), the relationship between the time course of the magainin 2 concentration in the GUV membrane and magainin 2-induced membrane permeation of AF647 was similar. Values of t_L decreased with an increase in CF-magainin 2/magainin 2 concentration (Figure 3E).

We also observed similar patterns of the increase in the rim intensity in the interaction of 6.2 μM CF-magainin 2/magainin 2 with 50%DOPG/50%DOPC-GUVs (see SI). In this case the rim intensities were larger than those for 40%DOPG/60% DOPC-GUVs because the fraction of CF-magainin 2 in 6.2 μM CF-magainin 2/magainin 2 (2.9 mol %) is much larger (Figure S6). Therefore, irrespective of magainin 2 concentration the time course of the rim intensity is similar.

The results in SI (Figure S7) indicate that the dissociation of CF-magainin 2 from the membrane into aqueous solution is rapid: the lifetime of the binding state is less than 30 s. This result clearly indicates that if the CF-magainin 2 molecules were present in the inner monolayer of the GUV, they would be rapidly dissociated into the aqueous solution inside the GUV. If the transfer of CF-magainin 2 from the outer to the inner monolayer occurs only once (i.e., after CF-magainin 2 in the inner monolayer moves to the GUV lumen, no new CF-magainin 2 is transferred from the outer to the inner monolayer), the concentration of CF-magainin 2 in the GUV lumen is very low, which cannot be measured. However, under the experimental condition using the single GUV method, the concentration of CF-magainin 2 in the outside of the GUV is kept constant, and thereby, new CF-magainin 2 in the inner monolayer can be continuously provided from the outside of the GUV via the transfer from the outer to the inner monolayer and the binding of CF-magainin 2 to the outer monolayer from the outside of the GUV. Hence, CF-magainin 2 can be transferred from the outside of the GUV to the GUV lumen continuously. In this case the concentration of CF-magainin 2 in the GUV lumen would increase significantly during the long period of constant rim intensity. However, we did not observe an increase in the fluorescence intensity in the aqueous solution inside the GUV before pore formation (e.g., Figure 3A(2) and

DOI: 10.1021/la503318z
Langmuir 2015, 31, 3391−3401

B(2)). Consequently, these results suggest that CF-magainin 2 cannot translocate from the outer to the inner monolayer until just before pore formation and that during the increase in rim intensity from I_1 to I_2 CF-magainin 2 translocates from the outer to the inner monolayer until the surface concentrations of CF-magainin 2 in the inner and outer monolayers are almost equal.

After pore formation in the membrane, magainin 2 molecules in the buffer outside of the GUV can enter the GUV by diffusion through the pore because the size of the initial pore induced by magainin 2 is larger than that of magainin 2 molecule.[22] However, in the case of the single GUV method, magainin 2 solution is continuously added into the vicinity of a GUV. Depending on the location of the pore in the GUV membrane, this flow of the magainin 2 solution increases the rate of the entry of magainin 2 into the GUV lumen. Thereby, the rapid entry of magainin 2 into the GUV lumen observed in Figure 3A (~144 s) and B (~290 s) may be due not to diffusion, but to flow. This consideration indicates that this rate is not useful for determining the rate of entry of magainin 2 into the GUV lumen through the pore.

3.4. Relationship of the Time Course of Magainin 2-Induced Change in the Area of the GUV Membrane, Magainin 2 Concentration in the GUV Membrane, And the Membrane Permeation of AF647. We simultaneously measured the magainin 2-induced change in the area, the increase in rim intensity, and the membrane permeation of AF647. A single 40%DOPG/60%DOPC-GUV containing AF647 was held at the tip of a micropipet A with a tension of 0.50 mN/m, and then CF-magainin 2/magainin 2 solution was continuously added from another micropipet B into the vicinity of the GUV (magainin 2 concentration in the outside of the GUV was 15 μM) (Figure 1A2). Concurrently, we observed the change in the area of the GUV and the fluorescence intensity of CF-magainin 2 and AF647 using CLSM (Figure 4A). Figure 4B shows that both the fractional change in the area and the rim intensity rapidly increased to a steady value within 50 s and then remained constant for a long time (~200 s) until pore formation. These time courses are almost the same and support the relationship $\delta = aX$, because the magainin 2 surface concentration is proportional to the rim intensity. The steady value of the fluorescence intensity was similar to that of the first steady value, I_1, of Figure 3D. We could not detect an increase in the rim intensity or that in fractional change in area just before pore formation. A similar result was obtained with 23 μM CF-magainin 2/magainin 2.

We also applied this method to the magainin 2-induced pore formation in the presence of a tension of 3 mN/m described in section 3.2. A single 40%DOPG/60%DOPC-GUV was held at the tip of a micropipet A with a tension of 0.50 mN/m for a few minutes and then a CF-magainin 2/magainin 2 solution was continuously added for 40 s from another micropipet B into the vicinity of the GUV (magainin 2 concentration in the outside of the GUV was 5.8 μM) to attain steady binding of magainin 2 to the membrane (i.e., the rim intensity became a maximum value). We then rapidly (~10 s) increased the aspiration pressure to a tension of 3.0 mN/m and held this tension for a specific time. Pore formation occurred stochastically, and the rim intensity or fractional change in area did not change before pore formation (Figure 4C).

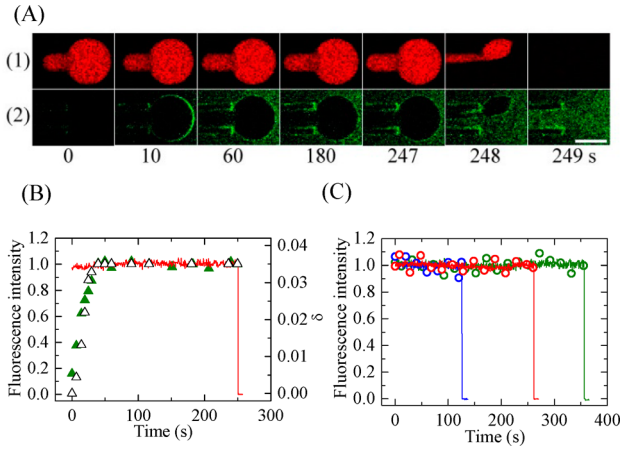

Figure 4. Time course of magainin 2-induced change in δ, magainin 2 concentration in the GUV membrane, and membrane permeation of AF647 in single 40%DOPG/60%DOPC-GUVs held at the tip of a micropipet. (A) CLSM images of (1) AF647 and (2) CF-magainin 2. A GUV held at 0.50 mN/m was interacted with 15 μM CF-magainin 2/magainin 2. The numbers below each image show the time in seconds after the initiation of CF-magainin 2/magainin 2 addition. The bar corresponds to 20 μm. (B) Time course of the change in fluorescence intensity of the GUV and fractional change in the area of GUV shown in (A). Red line represents the normalized fluorescence intensity of AF647 inside the GUV (left axis of B). Black open triangle represents δ, which is expressed as measured values (right axis of B). Green solid triangle represents the fluorescence of CF-magainin 2 in the rim of the GUV, which is expressed as normalized fluorescence intensity (left axis of B), FI = $I(t)/I_s$, where $I(t)$ and I_s are the fluorescence intensity of CF-magainin 2 in the rim of the GUV at time = t and the average fluorescence intensity at the steady state from 60 to 247 s. (C) Time course of the fluorescence intensity of the GUV membrane (circle), and the fluorescence intensity inside the GUV (solid line) held at 3.0 mN/m in the presence of 5.8 μM CF-magainin 2/magainin 2. Each color (solid line and circles) corresponds to the result of one GUV. The results of three GUVs are shown.

4. DISCUSSION

The results shown in this report clearly indicate that the stretch of a lipid membrane (i.e., the increase in δ) due to the binding of magainin 2 is the main driving force for magainin 2-induced pore formation, and that k_p greatly increases with an increase in the extension (or the area) of the lipid membrane. Moreover, tension due to an external force activates magainin 2-induced pore formation. These results indicate that the magainin 2-induced pore is a stretch-activated pore. On the other hand, it is well-known that some ion channel proteins form mechanosensitive channels whose probability of opening increases as the tension-induced stretch of the lipid membrane increases.[36] It is interesting to compare the characteristics of the stretch-activated pore produced by magainin 2 with that of mechanosensitive channels.

The results of Figures 3 and 4 revealed the following relationship between the location of magainin 2 and magainin 2-induced pore formation. At the beginning of the interaction of magainin 2 with single GUVs, magainin 2 molecules bind rapidly with the membrane interface of the outer monolayer, inducing an increase in the area of the GUV membrane. Steady binding was attained in less than 1 min, after which the surface concentration of magainin 2 and the area of the GUV membrane remained constant for an extended period of time (e.g., 40–240 s for 40%DOPG/60%DOPC-GUVs) until just before pore formation. At 4–32 s before the start of membrane

DOI: 10.1021/la503318z
Langmuir 2015, 31, 3391−3401

permeation of AF647, the rim intensity of GUVs started to increase rapidly and reached a second steady value. Membrane permeation began during this increase. There are three possible interpretations of this second increase in magainin 2 concentration and concomitant membrane permeation. The first interpretation (interpretation A) is that stretching of the inner monolayer induces pore formation in the bilayer, followed by the transfer of magainin 2 from the outer to the inner monolayer. The binding of magainin 2 in the outer monolayer increases the area of the outer monolayer, which causes the inner monolayer to stretch so that the two monolayers maintain the same area (see below). This stretching induces pore formation in the bilayer stochastically. It is believed that a stretching-induced pore has a toroidal structure where the outer monolayer connects to the inner monolayer.[14,37,38] At the initial stage of pore formation (i.e., before 140 s in Figure 3C and 267 s in D), the pore radius increases from zero, and therefore the radius of the pore is too small for AF647 to pass through the pore (i.e., no leakage occurs). When the pore size becomes larger than the diameter of magainin 2 (i.e., at 140 s in Figure 3C and 267 s in D), magainin 2 molecules bound to the outer monolayer can diffuse into the inner monolayer via the wall of the toroidal structure.[26−28] Lipids in a membrane in the liquid-crystalline phase have a high lateral diffusion coefficient,[39] and this reasonably explains the rapid diffusion (less than 30 s) of a magainin 2 molecule bound to several lipids. This interpretation indicates that the increase in the rim intensity is due to the diffusion of magainin 2 from the outer to the inner monolayer through the initial pore wall. After the radius of the pore increases to a certain larger size, AF647 starts to leak (i.e., at 149 s in Figure 3C and 297 s in D). Therefore, there is a time lag between the time when the rim intensity starts to increase and the start of membrane permeation of AF647 (i.e., t_L). The increase in magainin 2 concentration causes the tension in the inner monolayer to increase, which increases the rate of opening (i.e., the increase in the radius) of the magainin 2-induced pore. Therefore, t_L decreases with an increase in magainin 2 concentration (Figure 3E).

The second interpretation (interpretation B) is that stretching of the inner monolayer induces transfer of magainin 2 from the outer to the inner monolayer stochastically, followed by pore formation. Huang and colleagues reported that the transfer of melittin from the outer to the inner monolayer occurs before the leakage of water-soluble dye (i.e., the formation of stable pores), and that leakage began when the membrane area increased by 3.4%.[34] According to their theory, the binding of melittin to both the outer and inner monolayers stretches the lipid bilayer, which increases membrane strain as the protein to lipid ratio increases, and a stable pore forms at a critical value of strain to decrease the free energy of the strain. The transfer of transportan 10 (TP10) from the outer to the inner monolayer occurs before the leakage of water-soluble dye, although measurements of the amount of peptide transferred prior to pore formation obtained by different techniques and different laboratories differ.[23,35] It is noteworthy that melittin induced pore formation in GUVs fixed at the tip of micropipet using a small suction pressure when the increase in area reached a critical value.[34] In contrast, magainin 2 did not induce pore formation when the change in area reached a critical value, but after maintaining this critical change in area for an extended period of time, pore formation occurred stochastically (Figure 4B). It is well-known that stretching of lipid membranes induces fluctuation of the density of lipids in the membrane.[14,30] When the degree of this fluctuation becomes a critical value transiently, magainin 2 molecules transfer from the outer to the inner monolayers and then pore formation occurs. Two-sided binding of magainin 2 likely plays an important role in pore formation in interpretation B. On the other hand, tension caused by an external force results in no increase in rim intensity just before the start of leakage (Figure 4B and C). This result cannot be explained by interpretation B because pore formation is not possible without the transfer of magainin 2 from the outer to the inner monolayer in this interpretation. However, this result can be explained by interpretation A as follows: the tension caused by the aspiration of a GUV by a micropipet increases the rate of opening (i.e., the increase in the radius) of the magainin 2-induced pore and hence the GUV is immediately aspirated into the micropipet after pore formation starts.

The third interpretation (interpretation C) is that a conformational change of magainin 2 induces pore formation. After magainin 2 binds to the membrane interface of the outer monolayer parallel with the membrane surface,[7] magainin 2 undergoes a conformational change resulting in pore formation; for example, magainin 2 may adopt a bilayer-spanning conformation, forming a pore. A similar conformational change is observed in alamethicine.[40,41] However, in interpretation C, the conformational change of magainin 2 does not induce an increase in its concentration in a GUV membrane, and therefore the fluorescence intensity due to CF-magainin 2 would not increase just before leakage of AF647. This contradicts our experimental result (see Figure 3). Therefore, interpretation A is the most plausible of the three interpretations.

The experimental results strongly indicate that magainin 2 cannot translocate from the outer to the inner monolayer until just before formation of the initial pore. Therefore, there are no magainin 2 molecules in the inner monolayer until just before the intact GUV is disrupted. α-Helical magainin 2 molecules bind and penetrate the interface of the outer monolayer due to the high interfacial hydrophobicity.[20,33] This increases the area of the outer monolayer (i.e., the outer monolayer stretches) mainly due to steric repulsion between the hard, incompressible α-helices and the hydrophilic segments of the lipids. The flip-flop of phospholipids is a slow process, with a half time on the order of several hours,[42] so there is likely negligible transfer of phospholipid from the outer to the inner monolayer during the experimental time scale (~6 min). The spherical shape of the GUV did not change during the interaction of magainin 2 with a GUV, and so the area of the inner monolayer remained the same as that of the outer monolayer. Woo et al. investigated the interaction of magainin 2 with lipid bilayers of a mixture of dipalmitoyl-PC (DPPC) and palmitoyloleoyl-PG (POPG) using coarse-grained simulation and found that the binding of magainin 2 to only one monolayer in the bilayer induces buckling of the bilayer and vesicle budding.[43] However, we did not observe such local changes in the shape of GUVs within the spatial resolution of microscopy.[20,21] Moreover, the results of the present study clearly provide direct evidence that the binding of magainin 2 induces an increase in the area of the bilayer (Figure 1) and strongly indicate that the area of the inner monolayer increases, i.e., the monolayer stretches. The stretching of the inner monolayer induces positive tension in the inner monolayer; this positive tension in a monolayer tends to decrease the area of the monolayer and counterbalances the

DOI: 10.1021/la503318z
Langmuir 2015, 31, 3391−3401

external tension induced by the increase in the area of the outer monolayer.[22] It is well-known that the stretching of lipid membranes induced by an external force induces pore formation as a result of thermal fluctuation of the lipid membrane lateral density.[14,30,37,38] Generally, the lateral tension in a monolayer, σ_m, is proportional to the fractional change in the area of the monolayer δ (i.e., $\sigma_m = 1/2 \cdot K_A \delta$, where K_A is the elastic compressibility modulus of the bilayer). Using the value of K_A obtained for 40%DOPG/60%DOPC-GUVs ($K_A = 141 \pm 5$ mN/m; for further details, see SI), we can calculate the lateral tension in the inner monolayer of the GUV, σ_{in} ($= 1/2 \cdot K_A \delta$). X can be converted to σ_{in} using $\delta = 0.58X$: $\sigma_{in} = 70.5\delta = 41X$ mN/m. Figure 1D shows that for 40%DOPG/60%DOPC-GUVs, the value of k_p greatly increased from 3.5×10^{-3} to 4.8×10^{-2} s^{-1} with an increase in X from 0.071 to 0.082 mol/mol, which corresponds to an increase in σ_{in} from 2.9 to 3.4 mN/m. Recently, we investigated tension-induced pore formation in 40%DOPG/60%DOPC-GUVs under the same buffer conditions as used in the present report; pore formation was induced by a constant external tension produced by micropipet aspiration.[30] The results showed that a constant tension of between 6 to 7 mN/m (which corresponds to 3.0 to 3.5 mN/m in each monolayer) induced pore formation with rate constants of between 4.9×10^{-3} and 1.9×10^{-2} s^{-1}. These values for the tension in a monolayer are similar to those of σ_{in} in magainin 2-induced pore formation, suggesting that the increase in σ_{in} due to the adsorbed magainin 2 in the outer monolayer plays a key role in magainin 2-induced pore formation.

Several researchers investigated the effects of "stretching" on peptide-induced pore formation. Huang et al. investigated the interaction of peptides such as melittin with oriented multilayers using X-ray diffraction and oriented circular dichroism and found that membrane thickness decreased with an increase in peptide concentration.[44−46] According to their investigations, the peptide to lipid ratio, P/L, is an important factor for pore formation because it may play a vital role in membrane tension. The membrane thickness decreases linearly with P/L and reaches a steady value when P/L exceeds a critical value $(P/L)^*$. They also detected transmembrane peptides only if $P/L > (P/L)^*$. Based on these results, they proposed the two-phase model (originally the two-state model) for pore formation: the S phase where peptides bind to the membrane interface, and the I phase which is composed of monodisperse oligomeric states of peptides.[44−47] In their model, the two phases are in equilibrium, and they obtained the threshold concentration of peptide required for pore formation using the physical principle that the chemical potentials of lipid in both phases are equal.[46] Thus, the transition, from a state of no pores (S phase) to a state of multiple pores (I phase) of the same size, as a function of P/L resembles a phase transition. Initially, they assumed that the observed membrane stretching and thinning was due to the distribution of adsorbed peptides in both monolayers of the oriented multilayers, but later confirmed that melittin induced the increase in area in the GUV membrane due to the distribution of adsorbed peptides to both monolayers, since melittin can easily translocate from the outer to the inner monolayer.[34] Therefore, their theory reasonably explains pore formation induced by peptides such as melittin. On the other hand, for magainin 2-induced pore formation, we proposed a model for an irreversible two-state transition: from an intact GUV (i.e., nonleaky GUV) state where magainin 2 molecules are bound to the membrane interface of the outer monolayer, to the pore state through which the internal contents of the GUV are leaking or have completely leaked (i.e., leaking or leaked GUV). This model explains the stochastic pore formation in single GUVs; using this model, we obtained the rate constant of the two-state transition from the intact state to the pore state.[20] The pore state in our model is not an equilibrium state, as supported by the experimental results showing that the pore size changes over time during the pore state.[22] The results in the present report show that magainin 2 can bind to only the outer monolayer, causing an increase in the area of the bilayer. This area then remains constant for a considerable period of time. The data do not indicate that the peptides interact with both monolayers simultaneously.

In our previous report,[22] we proposed a new hypothesis that the binding of magainin 2 to the outer monolayer induces a stretching of the inner monolayer composed of pure lipids, which in turn induces stochastic pore formation. In this report we provided experimental evidence for this hypothesis. It is noteworthy that in the experiments shown in Figure 1ABC, the applied tension to the membrane remained constant, indicating that the tension in the outer monolayer did not increase during the area increase due to the binding of magainin 2. This result indicates that the binding of magainin 2 to the outer monolayer does not increase the tension in the bilayer but rather induces tension only in the inner monolayer. On the other hand, Leontiadou et al. described molecular dynamics (MD) simulations of the interaction between DPPC membrane and magainin 2-H2, an analogue of magainin 2 which can interact with electrically neutral membranes. Their findings indicated that the binding of magainin 2-H2 on the outer monolayer induces an increase in the area of the inner monolayer, and then induces the formation of a nanometer-sized, toroidal-shaped pore in the bilayer.[48] These findings support our results described in this report. The results in our previous report indicate that the size of the initial pore depends on the area of the lipid membrane.[22] In their simulation, Leontiadou et al. used 128 DPPC molecules and 4 magainin 2-H2 peptides, and so the area of the membrane was very small. If MD simulations could be conducted using a large number of lipids (i.e., corresponding to the number of lipids in a GUV) in future, the size of the initial pore observed in the simulation might increase.

Moreover, the results in Figure 2 indicate that the stretching of a lipid membrane (i.e., the inner monolayer) due to the binding of magainin 2 and the stretching due to the external force can be added together to increase the total tension (or stretching) in the inner monolayer, which determines the rate constant of pore formation (i.e., the additivity of tension or stretching). This can be generalized. If magainin 2 coexists with another peptide which binds with the outer monolayer to induce stretching, the rate constant of magainin 2-induced pore formation would increase. A recent report[49] that amyloid peptide and magainin 2 are cross-cooperative in the induction of leakage may be an example of this phenomenon.

5. CONCLUSION

In this report, we provide evidence for magainin 2-induced stretching of a lipid membrane and describe its relationship with the rate constant of a magainin 2-induced two-state transition from the intact state to the pore state, k_p. The results of confocal microscopy indicate that magainin 2 binds to the membrane interface of only the outer monolayer just before pore formation (i.e., asymmetric distribution). Based on the

DOI: 10.1021/la503318z
Langmuir 2015, 31, 3391−3401

results, we conclude that the stretching of the inner monolayer is a main driving force of magainin 2-induced pore formation, and that the rate constant of magainin 2-induced pore formation greatly increases as the stretch of the inner monolayer increases. To our knowledge, this is the first experimental evidence for the effects of stretching or the tension in the inner monolayer on pore formation of antimicrobial peptides in lipid membranes. Moreover, tension due to an external force activates magainin 2-induced pore formation. These results indicate that a magainin 2-induced pore is a stretch-activated pore.

■ ASSOCIATED CONTENT

Supporting Information

Determination of magainin 2 concentration in a vicinity of a single GUV using confocal microscopy, measurement of the fluorescence intensity of the rim of the GUV, and re-evaluation of the intrinsic binding constant of magainin 2 with the lipid membranes. This material is available free of charge via the Internet at http://pubs.acs.org.

■ AUTHOR INFORMATION

Corresponding Author

*E-mail: yamazaki.masahito@shizuoka.ac.jp. TEL and FAX: 81-54-238-4741.

Author Contributions

Mohammad Abu Sayem Karal, Jahangir Md. Alam, and Tomoki Takahashi contributed equally.

Notes

The authors declare no competing financial interest.

■ ACKNOWLEDGMENTS

This work was supported in part by a Grant-in-Aid for Scientific Research (B) (No. 21310080 in 2009-2012) from JSPS to M.Y., and also by a Grant-in-Aid for Scientific Research in Priority Areas (Soft Matter Physics) (No. 21015009 in 2009-2011) from the Ministry of Education, Culture, Sports, and Science to M.Y. Part of this work was carried out under the Cooperative Research Project of the Research Institute of Electronics, Shizuoka University.

■ REFERENCES

(1) Zasloff, M. Antimicrobial peptides of multicellular organisms. *Nature* **2002**, *415*, 389−395.

(2) Melo, M. N.; Ferre, R.; Castanho, A. R. B. Antimicrobial peptides: linking partition, activity and high membrane-bound concentrations. *Nat. Rev. Microbiol.* **2009**, *8*, 1−5.

(3) Hwang, P. M.; Vogel, H. J. Structure-function relationships of antimicrobial peptides. *Biochem. Cell Biol.* **1998**, *76*, 235−246.

(4) Zasloff, M. Magainins, a class of antimicrobial peptides from Xenopus skin: Isolation, characterization of two active forms, and partial cDNA sequence of a precursor. *Proc. Natl. Acad. Sci. U.S.A.* **1987**, *84*, 5449−5453.

(5) Zasloff, M.; Martin, B.; Chen, H.-C. Antimicrobial activity of synthetic magainin peptides and several analogues. *Proc. Natl. Acad. Sci. U.S.A.* **1988**, *85*, 910−913.

(6) Wade, D.; Boman, A.; Wahlin, B.; Drain, C. M.; Andreu, A.; Boman, H. G.; Merrifield, R. B. All-D amino acid-containing channel-forming antibiotic peptides. *Proc. Natl. Acad. Sci. U.S.A.* **1990**, *87*, 4761−4765.

(7) Bechniger, B.; Zasloff, M.; Opella, S. J. Structure and orientation of the antibiotic peptide magainin in membranes by solid-state nuclear magnetic resonance spectroscopy. *Protein Sci.* **1993**, *2*, 2077−2084.

(8) Hirsh, D. J.; Hammer, J.; Maloy, W. L.; Blazyk, J.; Schaefer, J. Secondary structure and location of a magainin analogue in synthetic phospholipid bilayers. *Biochemistry* **1996**, *35*, 12733−12741.

(9) Matsuzaki, K.; Murase, K.; Fujii, N.; Miyajima, K. Translocation of a channel-forming antimicrobial peptide, magainin 2, across lipid bilayers by forming a pore. *Biochemistry* **1995**, *34*, 6521−6526.

(10) Matsuzaki, K.; Sugishita, K.; Ishibe, N.; Ueha, M.; Nakata, S.; Miyajima, K.; Epand, R. M. Relationship of membrane curvature to the formation of pores by magainin 2. *Biochemistry* **1998**, *37*, 11856−11863.

(11) Boggs, J. M.; Euijung, J.; Polozov, I. V.; Epand, R. F.; Anantharamaiah, G. M.; Blazyk, J.; Epand, R. M. Effect of magainin, class L, and class A amphipathic peptides on fatty acid spin labels in lipid bilayers. *Biochim. Biophys. Acta* **2001**, *1511*, 28−41.

(12) Gregory, S. M.; Pokorny, A.; Almeida, P. F. F. Magainin 2 revisited: a test of the quantitative model for the all-or-none permeabilization of phospholipid vesicles. *Biophys. J.* **2009**, *96*, 116−131.

(13) Yamazaki, M. The single GUV method to reveal elementary processes of leakage of internal contents from liposomes induced by antimicrobial substances. *Advances in Planar Lipid Bilayers and Liposomes* **2008**, *7*, 121−142.

(14) Sandre, O.; Moreaux, L.; Brochard-Wyard, F. Dynamics of transient pores in stretched vesicles. *Proc. Natl. Acad. Sci. U.S.A.* **1999**, *96*, 10591−10596.

(15) Rawictz, W.; Olbrich, K. C.; McIntosh, T.; Needham, D.; Evans, E. Effect of chain length and unsaturation on elasticity of lipid bilayers. *Biophys. J.* **2000**, *79*, 328−339.

(16) Tanaka, T.; Yamazaki, M. Membrane fusion of giant unilamellar vesicles of neutral phospholipid membranes induced by La^{3+}. *Langmuir* **2004**, *20*, 5160−5164.

(17) Ambroggio, E. E.; Separovic, F.; Bowie, J. H.; Fidelio, G. D.; Bagatolli, L. A. Direct visualization of membrane leakage induced by the antibiotic peptides: maculatin, citropin, and aurein. *Biophys. J.* **2005**, *89*, 1874−1881.

(18) Domingues, T. M.; Riske, K. A.; Miranda, A. Revealing the lytic mechanism of the antimicrobial peptide gomesin by observing giant unilamellar vesicles. *Langmuir* **2010**, *26*, 11077−11084.

(19) Islam, M. Z.; Alam, J. M.; Tamba, Y.; Karal, M. A. S.; Yamazaki, M. The single GUV method for revealing the functions of antimicrobial, pore-forming toxin, and cell-penetrating peptides or proteins. *Phys. Chem. Chem. Phys.* **2014**, *16*, 15752−15767.

(20) Tamba, Y.; Yamazaki, M. Single giant unilamellar vesicle method reveals effect of antimicrobial peptide Magainin 2 on membrane permeability. *Biochemistry* **2005**, *44*, 15823−15833.

(21) Tamba, Y.; Yamazaki, M. Magainin 2-induced pore formation in membrane depends on its concentration in membrane interface. *J. Phys. Chem. B* **2009**, *113*, 4846−4852.

(22) Tamba, Y.; Ariyama, H.; Levadny, V.; Yamazaki, M. Kinetic pathway of antimicrobial peptide magainin 2-induced pore formation in lipid membranes. *J. Phys. Chem. B* **2010**, *114*, 12018−12026.

(23) Islam, M. Z.; Ariyama, H.; Alam, J. M.; Yamazaki, M. Entry of cell-penetrating peptide transportan 10 into a single vesicle by translocating across lipid membrane and its induced pores. *Biochemistry* **2014**, *53*, 386−396.

(24) Alam, J. M.; Kobayashi, T.; Yamazaki, M. The single giant unilamellar vesicle method reveals lysenin-induced pore formation in lipid membranes containing sphingomyelin. *Biochemistry* **2012**, *51*, 5160−5172.

(25) Tamba, Y.; Ohba, S.; Kubota, M.; Yoshioka, H.; Yoshioka, H.; Yamazaki, M. Single GUV method reveals interaction of tea catechin (−)-epigallocatechin gallate with lipid membranes. *Biophys. J.* **2007**, *92*, 3178−3194.

(26) Matsuzaki, K.; Murase, O.; Fujii, N.; Miyajima, K. An antimicrobial peptide, magainin 2, induced rapid flip-flop of phospholipids coupled with pore formation and peptide translocation. *Biochemistry* **1996**, *35*, 11361−11368.

DOI: 10.1021/la503318z
Langmuir 2015, 31, 3391−3401

(27) Ludtke, S. J.; He, K.; Heller, K. H.; Harroun, T. A.; Yang, L.; Huang, H. W. Membrane pores induced by magainin. *Biochemistry* **1996**, *35*, 13723−13728.
(28) Yang, L. T.; Weiss, M.; Lehrer, R. I.; Huang, H. W. Crystallization of antimicrobial pores in membranes: magainin and protegrin. *Biophys. J.* **2000**, *79*, 2002−2009.
(29) Tamba, Y.; Terashima, H.; Yamazaki, M. A membrane filtering method for the purification of giant unilamellar vesicles. *Chem. Phys. Lipids* **2011**, *164*, 351−358.
(30) Levadny, V.; Tsuboi, T.; Belaya, M.; Yamazaki, M. Rate constant of tension-induced pore formation in lipid membranes. *Langmuir* **2013**, *29*, 3848−3852.
(31) Evans, E. A.; Waugh, R.; Melnik, L. Elastic area compressibility modulus of red cell membrane. *Biophys. J.* **1976**, *16*, 585−595.
(32) Pataraia, S.; Liu, Y.; Lipowsky, R.; Dimova, R. Effect of cytochrome c on the phase behavior of charged multicomponent lipid membranes. *Biochim. Biophys. Acta* **2014**, *1838*, 2036−2045.
(33) Wimley, W. C.; White, S. H. Experimentally determined hydrophobicity scale for proteins at membrane interface. *Nat. Struct. Biol.* **1996**, *3*, 842−848.
(34) Lee, M. T.; Sun, T. L.; Hung, W. C.; Huang, H. W. Process of inducing pores in membranes by melittin. *Proc. Natl. Acad. Sci. U.S.A.* **2013**, *110*, 14243−14248.
(35) Wheaten, S. A.; Ablan, F. D. O.; Spaller, B. L.; Trieu, J. M.; Almeida, P. F. Translocation of cationic amphipathic peptides across the membranes of pure phospholipid giant vesicles. *J. Am. Chem. Soc.* **2013**, *135*, 16517−16525.
(36) Sachs, F. Stretch-activated ion channels: What are they? *Physiology* **2010**, *25*, 50−56.
(37) Evans, E.; Heinrich, V.; Ludwig, F.; Rawicz, W. Dynamic tension spectroscopy and strength of biomembranes. *Biophys. J.* **2003**, *85*, 2342−2350.
(38) Fuerties, G.; Giménez, D.; Esteban-Martin, S.; Sánchez-Muñoz, O. L.; Salgado, J. A lipocentric view of peptide-induced pores. *Eur. Biophys. J.* **2011**, *40*, 399−415.
(39) Almeida, P. F. F.; Vaz, W. L. C. Lateral diffusion in membranes, In *Structure and dynamics of membranes*; Lipowsky, R., Sackmann, E., Eds.; Elsevier Science B. V.: Amsterdam, 1995; pp 305−357.
(40) Sansom, M. S. Alamethicin and related peptaibols—model ion channels. *Eur. Biophys. J.* **1993**, *22*, 105−124.
(41) Bechinger, B. Structure and functions of channel-forming polypeptides: magainins, cecropins, melittin and alamethicin. *J. Membr. Biol.* **1997**, *156*, 197−211.
(42) Devaux, P. F.; Fellmann, P.; Hervé, P. Investigation on lipid asymmetry using lipid probes. Comparison between spin-labeled lipids and fluorescent lipids. *Chem. Phys. Lipids* **2002**, *116*, 115−134.
(43) Woo, H.-J. Wallqvist, Spontaneous buckling of lipid bilayer and vesicle budding induced by antimicrobial peptide magainin 2: A coarse-grained simulation study. *J. Phys. Chem. B* **2011**, *115*, 8122−8129.
(44) Lee, M.-T.; Chen, F.-Y.; Huang, H. W. Energetics of pore formation induced by membrane active peptides. *Biochemistry* **2004**, *43*, 3590−3599.
(45) Huang, H. W.; Chen, F.-Y.; Lee, M.-T. Molecular mechanism of peptide-induced pores in membranes. *Phys. Rev. Lett.* **2004**, *92*, 198304.
(46) Huang, H. W. Free energies of molecular bound states in lipid bilayers: lethal concentrations of antimicrobial peptides. *Biophys. J.* **2009**, *96*, 3263−3272.
(47) Lee, M.-T.; Hung, W.-C.; Chen, F.-Y; Huang, H. W. Mechanism and kinetics of pore formation in membranes by water-soluble amphipathic peptides. *Proc. Natl. Acad. Sci. U.S.A.* **2008**, *105*, 5087−5092.
(48) Leontiadou, H.; Mark, A. E.; Marrink, S. J. Antimicrobial peptides in action. *J. Am. Chem. Soc.* **2006**, *128*, 12156−12161.
(49) Last, N. B.; Miranker, A. D. Common mechanism unites membrane poration by amyloid and antimicrobial peptides. *Proc. Natl. Acad. Sci. U.S.A.* **2013**, *110*, 6382−6387.

DOI: 10.1021/la503318z
Langmuir 2015, 31, 3391−3401